Sum Frequency Generation Studies of Ammonium and Pyrrolidinium Ionic Liquids Based on the Bis-trifluoromethanesulfonimide Anion

Cesar Aliaga, Gary A. Baker, and Steven Baldelli*

Department of Chemistry, University of Houston, Houston, Texas 77204, and Oak Ridge National Laboratory, Oak Ridge, Tennessee 37831

Received: August 31, 2007; In Final Form: November 15, 2007

A systematic sum frequency generation vibrational spectroscopy study is conducted on the gas−liquid interface of room-temperature ionic liquids. The compounds contain ammonium and pyrrolidinium based cations, to which alkyl substituents of different length and/or functional groups are attached, and they are all combined with the bis-trifluoromethanesulfonimide anion ([imide]$^-$). The alkyl chain length shows a strong effect on the ordering of the chains at the topmost layer, reaching the maximum order for $(C_4H_9)N^+(CH_3)_2(C_3H_7)$ and $(C_6H_{13})N^+C_4H_8(CH_3)$. There is also evidence of gauche defects for longer alkyl chains, and changes in the spectral features for the shortest ones. The substitution of a carbon atom in the chain by oxygen, and its per-deuteration, provides the means to acquire a more complete description of the surface structure, and an unambiguous assignment of the vibrations detected in the SFG spectra. Finally, a brief comparison between alkylpyrrolidinium, and previously studied alkylimidazolium, cations is also established.

1. Introduction

Room-temperature ionic liquids (RTILs) are compounds formed by the combination of an organic cation and a weakly coordinating anion, organic or inorganic.[1−3] They possess unique physicochemical properties. Their low melting points enable them to form solventless liquid electrolytes, and in addition, they possess a relatively high conductivity, high thermal stability, wide electrochemical windows, and remain liquid for large temperature ranges.[2,4−6]

The interface chemistry of RTILs is still a relatively new and scarcely investigated subject, although some work exists on the properties of the gas−liquid, solid−liquid, and liquid−liquid interfaces.[7] The study of the gas−liquid interface is important, since the unique surface properties of room-temperature ionic liquids make them suitable for operations of flue gas scrubbing of atmospheric contaminants such as SO_2.[8,9] They possess potential for supercritical extraction operations due to the relatively high solubility of CO_2 in those compounds.[10,11] There is however a drawback; their relatively high viscosity compared with the traditional organic solvents limits the number of industrial applications. Therefore, the attention was focused on compounds with anions that can form RTILs with lower viscosity and lower melting points,[12] which involved the study of compounds based on anions such as triflate, bis(trifluoromethanesulfonyl)imide ([imide]$^-$), and dicyanamide ([DCA]$^-$).[4,12−16] This is due to the fact that the anion is usually responsible for dictating several of the physical properties of an ionic liquid.[17] However, the cations are also important; thus, the present investigation focuses on ionic liquids based on the alkylammonium and alkylpyrrolidinium cations combined with [imide]$^-$.

A number of different cations such as alkylimidazolium, alkylammonium, alkylsulfonium, pyrazinium, pyridinium, and pyrrolidinium have been paired with the [imide]$^-$ ion to form ionic liquids with different properties.[14,15,18−25] In addition, the weakly coordinating [imide]$^-$ causes a substantial depression in the melting point of the ionic liquids it forms, which is due in part to the charge delocalization that extends from the central nitrogen atom to the neighboring sulfur atoms, and less to the oxygen atoms, causing the charge to be buried inside the molecule. This, added to the shielding effect of the oxygen atoms and the terminal $-CF_3$ groups, reduces the Coulombic interactions with the cation, increasing the ion mobility and reducing the lattice energy.[4,26,27]

Aside from the amount of attention that imidazolium based ionic liquids have drawn as novel green solvents for chemistry,[3] alkylammonium and alkylpyrrolidinium cations have also been proposed as alternatives for a number of applications due to their properties. Alkylammonium cations, for instance, are sufficiently electrochemically stable to be used as supporting electrolytes, and their melting points approach room temperature as the overall size of the ammonium ion becomes large, and the asymmetry of the molecule increases.[25,28] Pyrrolidinium cations display similar characteristics and, in addition, possess higher conductivities in most of the cases.[29] They lie conceptually between the fully 3-dimensional quaternary ammonium cations and the close-to-planar imidazolium ions; some possess larger electrochemical windows compared with the ammonium based ones, and they are able to form ionic liquids that show plastic crystal behavior.[26,30,31] Finally, both alkylammonium and alkylpyrrolidinium cations have lower costs compared with imidazolium ions.[32]

The structures of the ionic liquids investigated in this work are shown in Figure 1. It is clearly seen that the cations possess relatively low symmetry, and that the substituent alkyl chain varies from 3 to 10 carbons for both ammonium and pyrrolidinium compounds. One of the pyrrolidinium imides has a methoxy-ethyl chain ([Py1(C2OC1)][imide]), and another one has a per-deuterated alkyl chain ([Py14D][imide]) as the substituents. This was performed in order to give unambiguous assignments of the vibrational modes observed in the sum frequency spectra. The results suggest that the ordering at the surface is maximum for the butyl substituted ammonium imide, and for the hexyl substituted pyrrolidinium imide, decreasing

10.1021/jp077008g CCC: $40.75
Published on Web 01/18/2008

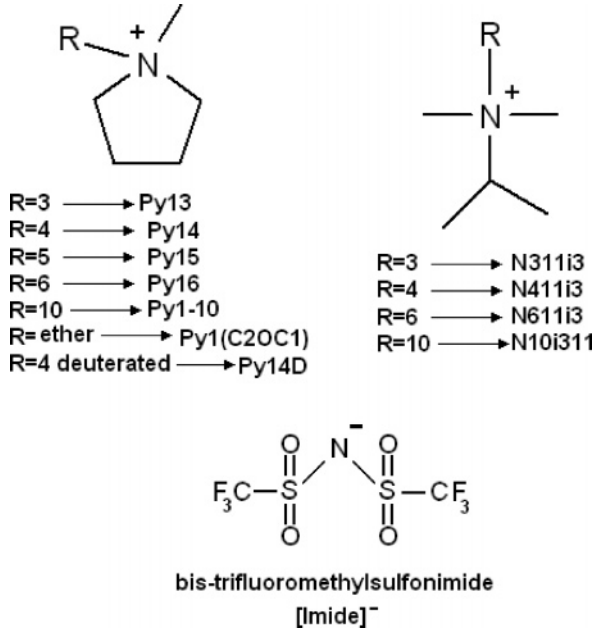

Figure 1. Structures of the ionic liquids investigated. The alkylpyrrolidinium cations are named as 1-methyl-1-alkylpyrrolidinium, and the alkylammonium compounds are named as dimethyl-isopropyl alkylammonium, for alkyl = propyl, butyl, pentyl, hexyl, and decyl. [Py1(C2OC1)] is 1-methyl-1-methoxyethyl pyrrolidinium.

for longer chains in every case. There is an increase in surface disorder proportional to the chain length as well.

Sum Frequency Generation (SFG). SFG is a second order nonlinear spectroscopy, sensitive to molecules in non-centrosymmetric environments. The SFG experiment consists of overlapping two high-intensity laser beams of frequencies ω_1 and ω_2, at the surface of a nonlinear medium which generates a second order nonlinear polarization $\boldsymbol{P}^{(2)}_{(\omega_1+\omega_2)}$ described by

$$\boldsymbol{P}^{(2)} = \chi^{(2)}:\boldsymbol{E}(\omega_{\mathrm{vis}})\boldsymbol{E}(\omega_{\mathrm{IR}}) \tag{1}$$

where $\boldsymbol{E}(\omega_i)$ is the electric field of the incoming beam and $\chi^{(2)}$ is the second order nonlinear susceptibility. The susceptibility has a nonresonant χ_{NR} and a resonant $\Sigma\chi_{\mathrm{R}}^{(2)}$ contribution. $\chi_{\mathrm{NR}}^{(2)}$ is a background contribution from the interface, and $\Sigma\chi_{\mathrm{R}}^{(2)}$ includes contributions from individual resonant modes $\chi_{\mathrm{R}}^{(2)}$. The expression for $\chi_{\mathrm{R}}^{(2)}$ is

$$\chi_{\mathrm{R}}^{(2)} = \left(\frac{N\langle\beta^{(2)}\rangle}{\omega_{\mathrm{IR}} - \omega_q + i\Gamma_q}\right) \tag{2}$$

where N is the number of modes contributing to the SFG signal, Γ_q is the damping constant for the qth vibrational mode with a frequency ω_q, ω_{IR} is the frequency of the incoming IR beam, and $\beta^{(2)}$ is the molecular hyperpolarizability averaged over all possible molecular orientations, and contains the Raman polarizability and the IR dipole transition moment. The intensity of the SFG signal is proportional to the square of the absolute value of the nonlinear polarization. It is thus evident that, whenever ω_q becomes comparable to ω_{IR}, the intensity of the signal is strongly enhanced, resulting in a peak in the spectrum.[33−35]

2. Experimental Section

Materials. 1-Iodobutane d_9 98% was purchased from Cambridge Isotope Laboratories. 1-Methylipyrrolidine >99+%, hexane anhydrous 99.8%, activated charcoal 60−100 mesh, and acetonitrile 99.5+% A.C.S. were purchased from Aldrich and were used as received. The water is deionized using a Millipore A10 system and has a resistivity of 18 MΩ·cm and a TOC index of <3 ppb.

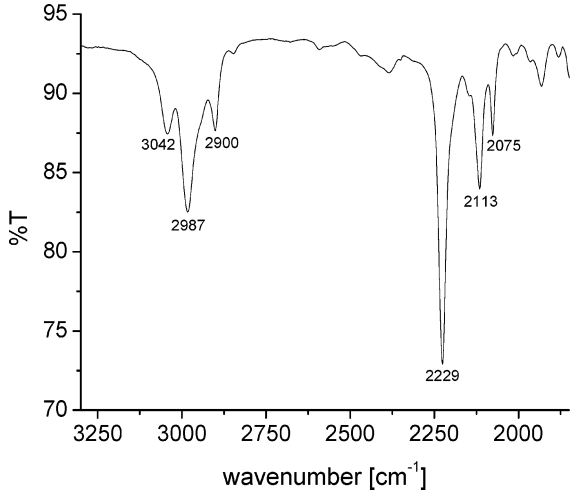

Figure 2. Infrared spectrum of [Py14D][imide].

Samples. The purity of the ionic liquids used in this study (Figure 1) was tested using ^{1}H NMR, UV−vis (to determine the cutoff), and fluorescence. All the samples but [N10i311][imide] were completely colorless and were used as received, which involves introducing them in the SFG cell and drying them in a vacuum line to a pressure of 5×10^{-5} Torr. The aforementioned 10-carbon ammonium sample was yellow and was diluted in ethanol and treated with activated charcoal for 4 h, filtered, dried in a rotary evaporator, transferred to the SFG cell, and dried in the vacuum line, which yielded a colorless liquid.

The deuterated compound was synthesized according to literature methods.[26] Iodobutane d_9 was added dropwise to a solution of methylpyrrolidine in acetonitrile, and the reacting mixture was refluxed at 70 °C overnight. The resulting yellow solid was washed three times with hexane, dissolved in water, and reacted with a solution of bis-trifluoromethanesulfonimide lithium salt. The resultant hydrophobic liquid was then washed several times with water, dried in a rotary evaporator, redissolved in ethanol, and treated with activated charcoal overnight several times. The solution was then filtered, dried in a rotary evaporator, filtered through a fine glass frit, transferred to the SFG cell, and dried in the vacuum line down to a pressure of 5×10^{-5} Torr. Once the desired pressure is reached, the cell is back-filled with dry argon to a slight overpressure, prior to being transferred to the SFG setup. [Py14D][imide] was characterized with ^{1}H NMR and Fourier transform infrared spectroscopy. The infrared spectrum is shown in Figure 2.

Spectroscopy System. The SFG spectrometer was described elsewhere.[36] It consists of an EKSPLA PL2143A/20 picosecond pulsed Nd:YAG laser with a 25 ps pulse and a 20 Hz repetition rate, whose 1064 nm output pumps an Optical Parametric Generation/Amplification system (Laser Vision, OPG/OPA). The fixed visible and the tunable infrared beams are collimated and overlap at the surface of the liquid following a copropagating geometry, with angles (with respect to the surface normal) of 50° for the visible and 60° for the IR. The SFG signal is finally sent to a gated integrator and collected in a computer program.

Data Collection and Analysis. The frequency of the IR laser beam is scanned at a rate of 1 cm^{-1}/s. Each data point corresponds to 20 averaged laser shots. Five spectra per

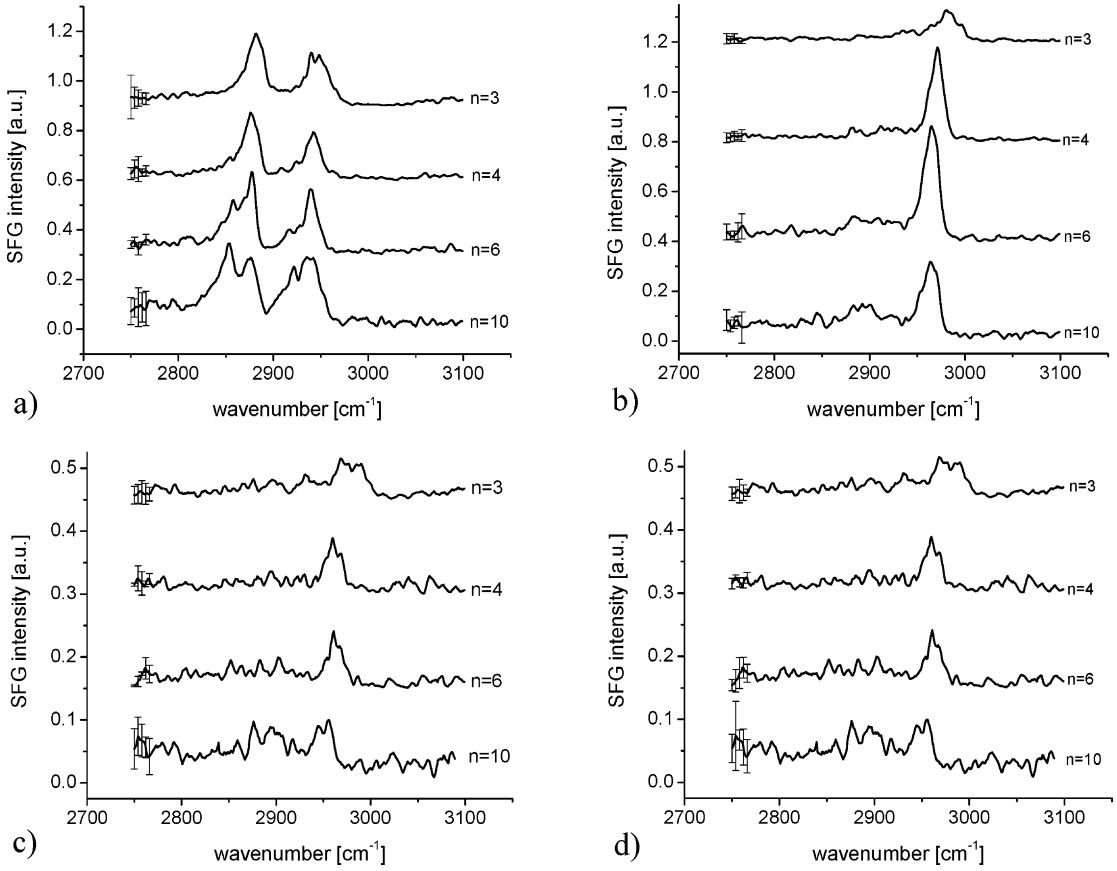

Figure 3. Sum frequency spectra of alkylammonium imides at polarization combinations ssp (a), ppp (b), sps (c), and pss (d). The offsets are 0.3, 0.4, 0.15, and 0.15 au, respectively.

TABLE 1: Vibrational Assignments for All Modes

vibration	wavenumber (cm^{-1})
r^+: symmetric methyl stretch	$2870-2880$[37−43]
r^-: asymmetric methyl stretch	$2960-2970$[37,38,40,42,43]
r^+_{FR}: methyl Fermi resonance	$2931-2942$[37,39,41−43]
d^+: symmetric methylene stretch	$2845-2858$[37,39,41−46]
d^-: asymmetric methylene stretch	~ 2910[41,44−48]
d^+_{FR}: methylene Fermi resonance	~ 2920[37,40,41,44,46]
r^+_{OMe}: symmetric methyl stretch in $O-CH_3$	~ 2828[43,49]
$r^+_{FR\_OMe}$: symmetric methyl in $O-CH_3$ Fermi resonance	~ 2930[43,49]
r^+_{NMe}: symmetric methyl stretch in $N-CH_3$	~ 2952[50]
r^-_{NMe}: asymmetric methyl stretch in $N-CH_3$	~ 3035[50]
r^+_D: methyl symmetric stretch C−D	~ 2059[43,51]
r^+_{DFR}: methyl symmetric stretch Fermi resonance C−D	~ 2113[43,51]
r^-_D: methyl asymmetric stretch C−D	~ 2209[51]

polarization combination are obtained, and the average is plotted along with error bars. The data are corrected for fluctuations in the infrared beam by dividing the averaged spectrum by data collected using gold as a substrate. The spectra are then fitted using eq 2 and Origin 6.0 software, utilizing a nonlinear fitting subroutine. The fitting is carried out using instrumental setting, which in addition to the error in the fit takes into consideration the error due to the scattering of the experimental points.

3. Results

The region pertaining to C−H vibrations is scanned in an interval ranging from 2750 to 3100 cm^{-1}. The vibration assignments are summarized in Table 1.

Ammonium Imides. Spectra for the alkylammonium imides are shown in Figure 3 for alkyl chain lengths corresponding to propyl, butyl, hexyl, and decyl. The spectra for a same polarization combination are shown, offset, in the same plot. In ssp polarization, all of the compounds show vibrations corresponding to d^+, d^+_{FR}, r^+, and r^+_{FR}, with the latter two being the most intense. Only [N311i3][imide] shows an additional feature corresponding to r^+_{NMe} at 2952 cm^{-1} with an amplitude similar to the r^- peak, and which disappears completely for the other compounds. In addition, the d^+ vibration, though very weak for shorter chains, increases in amplitude as the chain length increases, surpassing the r^+ peak for [N10i311][imide].

In ppp polarization, the dominating peak corresponds to the asymmetric methyl stretch (r^-). Only [N311i3][imide], besides showing a slight shift to higher frequency, evidences the r^+_{NMe} vibration at approximately 2959 cm^{-1}, appearing as a shoulder to the r^- peak. The r^+_{NMe} peak disappears completely as soon as one additional CH_2 unit is added to the chain. Similarly, the vibration corresponding to d^-, whose amplitude is very small for the shorter chains, increases appreciably as the alkyl chain becomes longer. Results for polarizations sps and pss also show

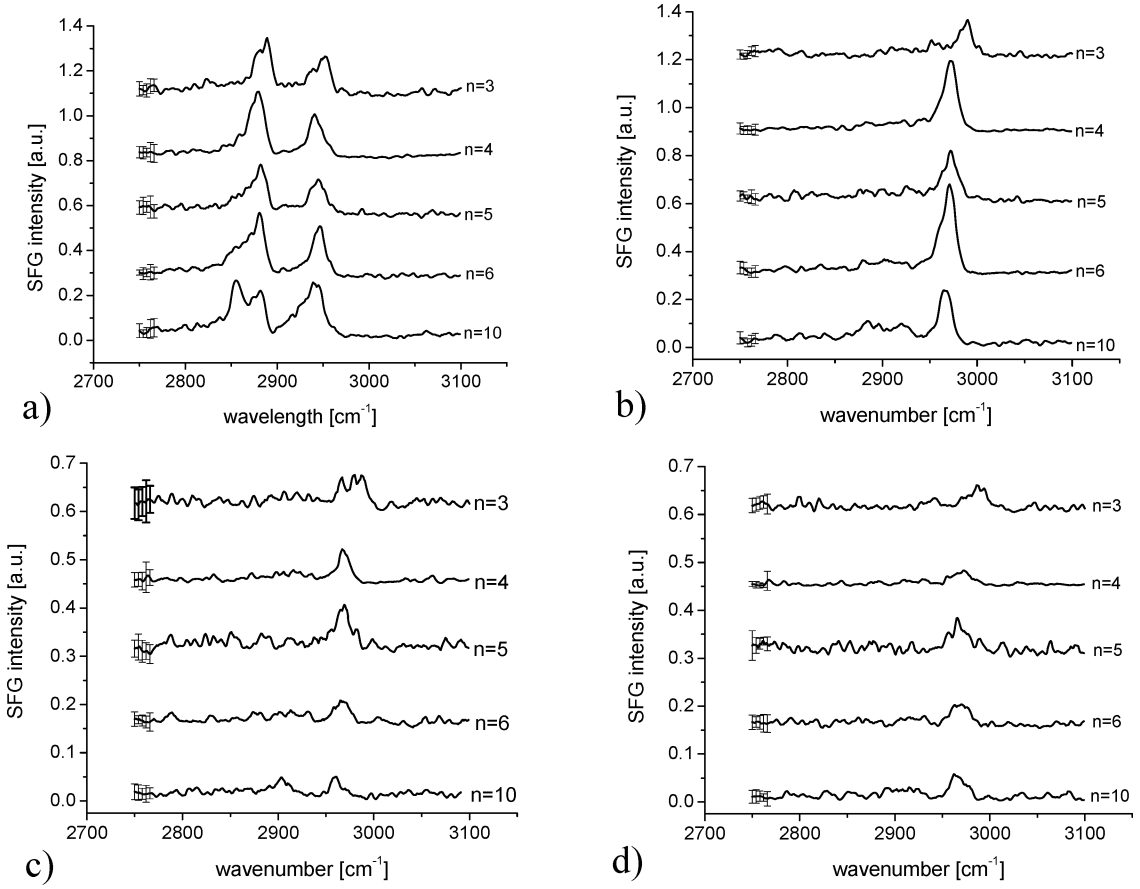

Figure 4. Sum frequency spectra of alkylpyrrolidinium imides at polarization combinations ssp (a), ppp (b), sps (c), and pss (d). The offsets are 0.27, 0.3, 0.15, and 0.15 au, respectively.

TABLE 2: Summary of the Spectroscopy Results for the Ammonium Imides at ssp and ppp Polarization Combinations (The Abbreviations Describe the Strength of the Band: n/d = Nondetectable, n/l = Noise Level, w = Weak, m = Medium Strength, s = Strong)

	ssp				ppp			
	N311i3	N411i3	N611i3	N10i311	N311i3	N411i3	N611i3	N10i311
d^+	n/d	w	s	s	n/d	n/d	n/d	n/d
r^+	s	s	s	s	nl	nl	nl	w
d^-	w	w	w	w	n/d	n/d	nl	w
d^+_{FR}	w	m	n/d	n/d	n/d	n/d	n/d	n/d
r^+_{FR}	s	s	s	s	w	w	w	n/d
r^+_{NMe}	s	n/d	n/d	n/d	m	n/d	n/d	n/d
r^-	n/d	n/d	n/d	n/d	s	s	s	s

the r^- peak as the most intense one, and a small contribution from d^-, although inside the noise level. A peak corresponding to r^+_{NMe} appears only for [N311i3][imide]. The results for ssp and ppp polarization combinations are summarized in Table 2.

Pyrrolidinium Imides. The spectra of alkylpyrrolidinium imides, with chains consisting of propyl, butyl, pentyl, hexyl, and decyl, are shown in Figure 4. The spectra in ssp polarization show the vibrations d^+, r^+, d^-, and r^+_{FR}, while [Py13][imide] also contains a vibration corresponding to r^+_{NMe} at 2952 cm^{-1}. Similarly to the alkyl ammonium case, the amplitude of the peak corresponding to the d^+ vibration increases with the alkyl chain size, surpassing the r^+ peak for the 10-carbon alkyl chain. The d^- peak also increases, although to a much lesser extent as compared with d^+. Spectra in ppp polarizations show features similar to those displayed by the alkylammonium imides. Polarizations sps and pss also show resemblance, except for the peak corresponding to d^-, whose amplitude increases to a greater extent.

Two additional pyrrolidinium compounds were investigated. The first one ([Py1(C2OC1)][imide]) contains a methoxy-terminated group. This is intended to eliminate the contribution from methylene and methyl groups from the alkyl chain through the influence of the oxygen atom, strategically located in the chain. The ssp spectrum (Figure 5) shows bands that correspond to r^+_{OMe}, its Fermi resonance, and d^-. The plot in ppp polarization (weak signal) shows peaks corresponding to d^+ and r^-_{NMe}. It was not possible to detect any features for sps and pss. It is evident that the vibrations corresponding to normal methyl and methylene stretches were eliminated.

The last compound contains a butyl d_9 chain ([Py14][imide]), in order to completely eliminate any C−H contribution from it. The SFG spectra (Figure 6) were acquired in two different regions: 2000−2300 cm^{-1} for the C−D stretch and 2750−3100 cm^{-1} for the C−H stretch. The amount of SFG signal generated in this system is very low, for which reason the spectra were averaged over 20 scans. The spectra in the C−D region show vibrations corresponding to the r^+_D, r^-_D, and r^+_{DFR} modes in ssp and only r^-_D in ppp. The C−H region contains peaks corresponding to d^- and r^+_{NMe} (ssp) and d^- and r^-_{NMe} (ppp). Again, it is evident that methyl and methylene contributions

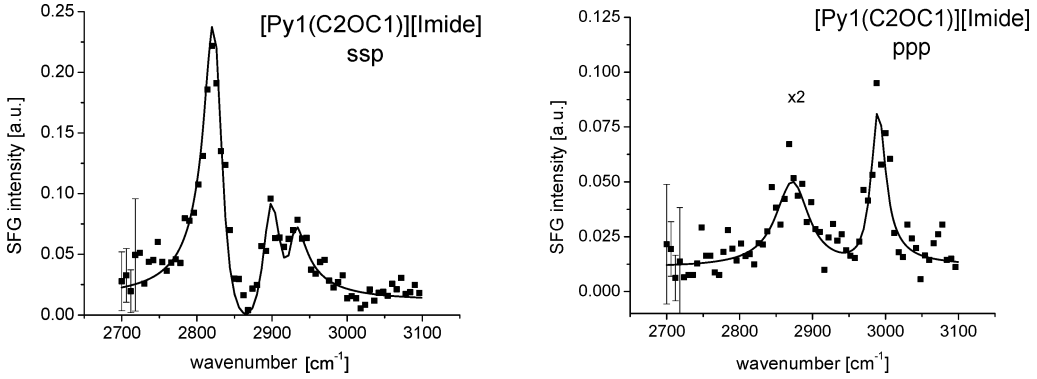

Figure 5. Sum frequency spectra of [Py1(C2OC1)][imide] at ssp and ppp polarization combinations.

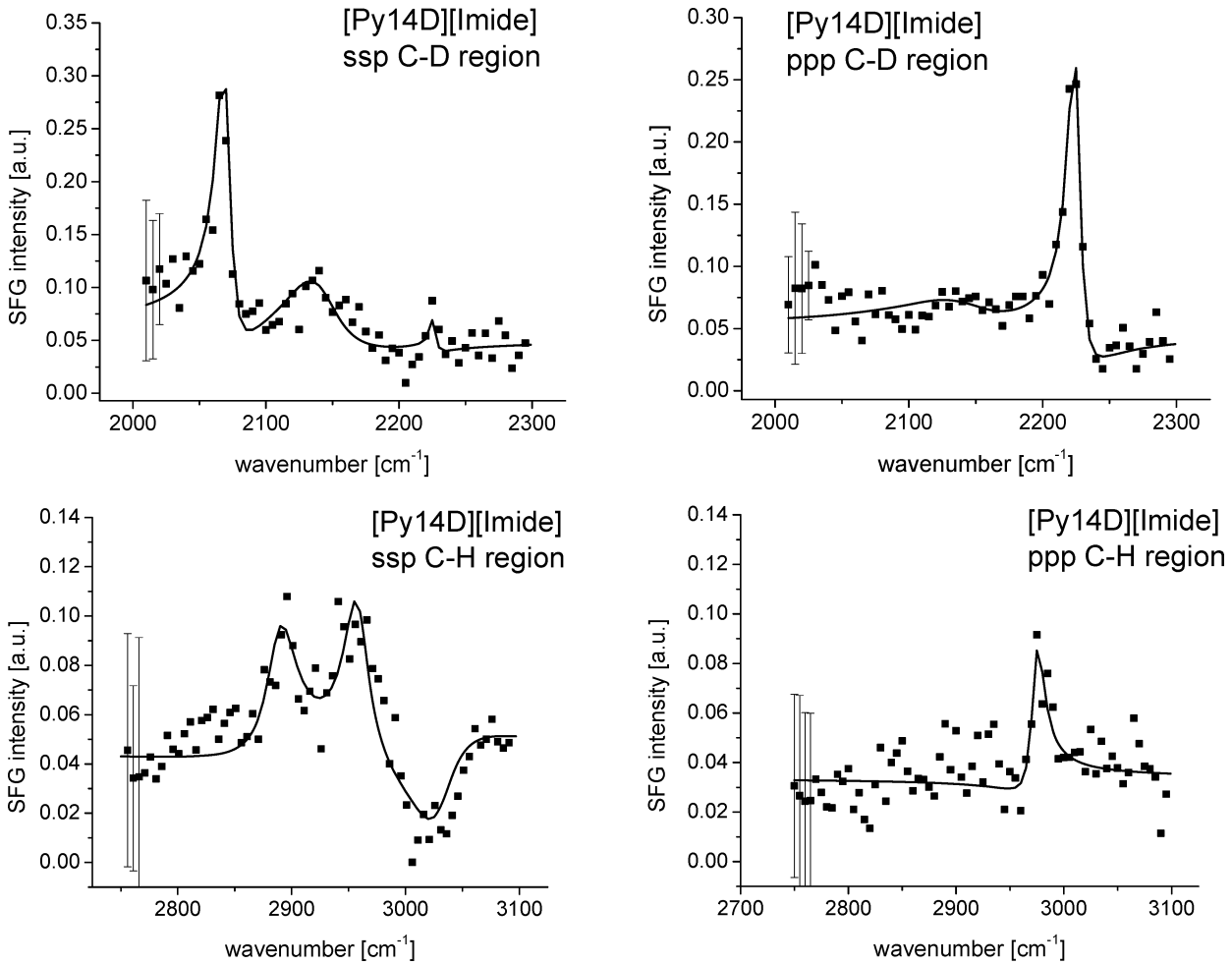

Figure 6. Sum frequency spectra of [Py14D][imide] at ssp and ppp polarization combinations, and two different regions (C−D and C−H stretch).

from the alkyl chain were eliminated. The results for ssp and ppp polarizations are summarized in Table 3.

TABLE 3: Summary of the Spectroscopy Results for the Pyrrolidinium Imides at ssp and ppp Polarization Combinations (The Abbreviations Describe the Strength of the Band: n/d = Nondetectable, n/l = Noise Level, w = Weak, m = Medium Strength, s = Strong)

	ssp					ppp				
	Py13	Py14	Py15	Py16	Py110	Py13	Py14	Py15	Py16	Py110
d^+	n/d	w	m	s	s	n/d	n/d	n/d	n/d	n/d
r^+	s	s	s	s	s	n/d	n/d	n/d	n/d	m
d^-	w	w	w	w	m	n/l	n/l	n/l	n/l	m
r^+_{FR}	s	s	s	s	s	n/d	n/l	n/l	n/d	n/d
r^+_{NMe}	s	n/d	n/d	n/d	n/d	m	n/d	n/d	n/d	n/d
r^-	n/d	n/d	n/d	n/d	n/d	s	s	s	s	s

4. Discussion

Peak Assignments for the Pyrrolidinium Imides. A major goal of this project is to understand the arrangement of ions at the surface of the ionic liquid. This involves locating how the charge center and the alkyl chains are oriented at the interface. For the alkylpyrrolidiniums, this entails the $N-CH_3$ moiety, and the ring methylene modes, which are good reporters of this, since they are rigidly attached to the positive charge on the nitrogen atom, and the terminal methyl group from the aliphatic substituents.

In order to discriminate between the vibrations coming from the pyrrolidinium ring and those originating at the alkyl chain, sum frequency spectra corresponding to [Py1(C2OC1)][imide] and [Py14D][imide] were obtained. As a first observation, the low signal-to-noise ratio and the weakness of the SFG signal

that characterize the spectra for the above-mentioned molecules are an indication that the main contribution comes from the alkyl chains, since [Py14][imide] generates a strong signal, with higher signal-to-noise ratio.

The spectra of [Py1(C2OC1)][imide] in Figure 5 show that the introduction of an oxygen atom in the butyl chain eliminates completely the vibrations corresponding to r^+, r^+_{FR}, r^-, d^+, d^+_{FR}, and $d^-$from the alkyl chain, leaving only those corresponding to the methoxy group, and the methylene groups from the ring. The ssp spectrum contains peaks corresponding to r^+_{OMe}, d^-, and $r^+_{FR\_OMe}$. And the ppp spectrum contains contributions from d^+ and r^+_{NMe}. This seemingly beneficial introduction of an oxygen atom in the aliphatic chain may nevertheless introduce some additional interactions caused by the presence of the heteroatom, such as hydrogen bonding, ion−dipole, and dipole−dipole, which could induce changes in the molecular structure at the surface.[52,53]

The experiment with the deuterated compound aims at eliminating this ambiguity by removing any possibility of additional interactions by using a fully deuterated version of the alkyl chain, due to the chemical similarity between the hydrogen and deuterium atoms. The results in Figure 6 (for a four carbon chain) show that the only contributions in ssp polarization belong to the asymmetric methylene stretch from the ring (d^-) and r^+_{NMe}, which suggests that, for [Py1(C2OC1)][imide], the methoxy group vibrations may have been masking the weak signal originating from $N-CH_3$ which is shown in Figure 4a. The ppp polarization differs from the preceding case by the absence of a peak corresponding to d^+, which was evident for [Py(C2OC1)][imide]. This suggests that the addition of an oxygen atom in the aliphatic chain changes the molecular structure at the interface.

It is suggested therefore that the presence of a peak pertaining to d^- in the pyrrolidinium compound spectra includes a contribution from the ring methylene vibrations, since it remains, after the elimination of all methylene contributions from the alkyl chain by the selective deuteration.

Orientation Calculations and Structure at the Interface. The orientation of the cation is derived from the polarization dependence of the sum frequency spectra, as described by Hirose et al.[54−56] and Wang et al.[57,58] who used the bond additivity model as an approximation. The terminal methyl groups of the alkyl chains are assigned C_{3v} symmetry and possess free rotation around the C_3 symmetry axis, therefore having an orientation described by the tilt angle θ (see Figure 7).

The polarization dependence compares the ratio of peak intensities of different vibrational modes with theoretical curves of peak intensity ratio versus orientational angle. Simulation curves of peak intensity ratios versus orientational angle θ as a function of the orientational distribution width σ were constructed and plotted simultaneously with the experimental peak ratios obtained from the fits of the spectra. A Gaussian expression $f(\theta)$ around a central orientation angle θ_m was adopted for the distribution.[59,60]

$$f(\theta) = \frac{1}{\sqrt{\pi/2}\sigma} e^{-(\theta-\theta_m)^2/2\sigma^2} \sin(\theta) \qquad (3)$$

From such analysis, a range of possible tilt angles for the symmetry axis of the chemical group under analysis with respect to the surface normal was obtained. In order to make use of the theoretical curves, the amplitude of the peak (A) is divided by its width (Γ), and the ratio is squared $(A/\Gamma)^2$. The orientation curves for the ammonium based and pyrrolidinium based ionic liquids are presented in Figure 8, where the orientational angle is plotted versus the chain length.

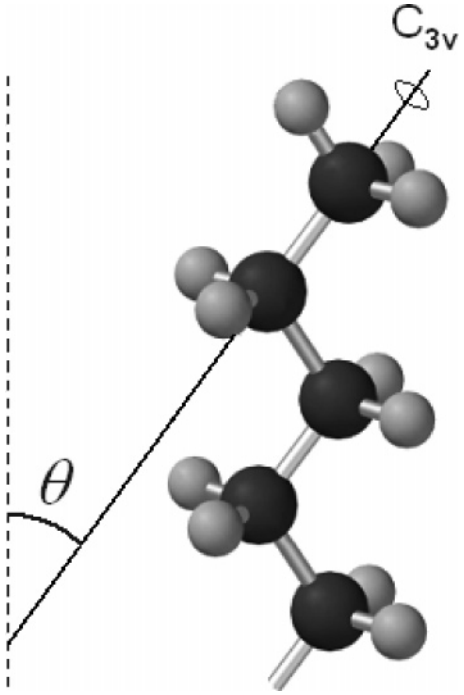

Figure 7. Representation of the tilt angle of an alkyl chain.

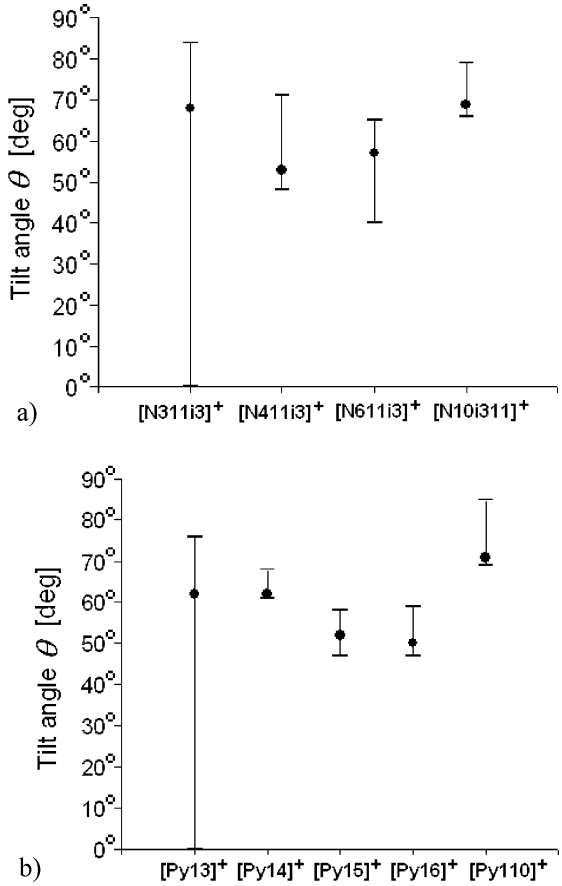

Figure 8. Molecular orientation dependence on the alkyl chain length for the ammonium and pyrrolidinium based ionic liquids. The angles are plotted along with the distribution.

The first observation regarding the interfacial structure comes from the difference in the spectra of [Py13][imide] and [N311i3][imide] compared to the rest of the compounds with longer alkyl

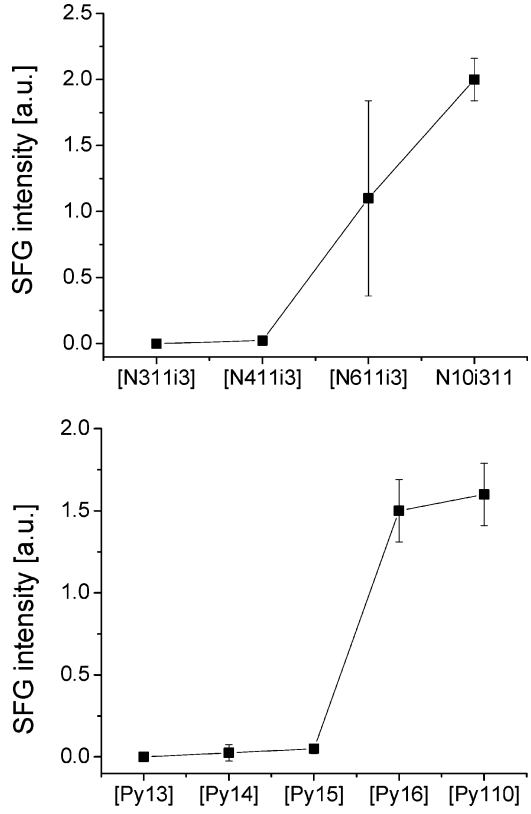

Figure 9. Peak amplitudes for the methyl symmetric stretch vibration of ammonium and pyrrolidinium imides.

chains. The peak corresponding to r^+_{NMe} in ssp and r^-_{NMe} in ppp for pyrrolidinium and ammonium imides is present only for the propyl case, which is clearly visible in the ssp spectra in Figures 3a and 4a. This suggests a poor molecular packing of the propyl chains at the surface, making the contribution of the $N-CH_3$ vibrations visible. For longer chains, lyophobic interactions apparently create a better packing, causing the vibrations from $N-CH_3$ to be no longer visible, as pointed by the fact that the $N-CH_3$ peaks disappear completely after a single additional CH_2 unit is added to the chain.

Plots of tilt angle versus the carbon chain length for each compound are shown in Figures 8 and 9. The asymmetric error bars correspond to the distribution in the tilt angle θ, calculated using eq 3, and originate from the calculation procedure: Even though the error bars for the peak amplitude ratios are symmetrical, once they are converted into tilt, the multiple curves associated with the distribution create the asymmetry. For the ammonium imides, $[N311i3]^+$ shows a very large distribution interval, which is likely due to the peak corresponding to r^+_{NMe}, being adjacent to the r^+_{FR}, which interferes with the analysis procedure. The minimum tilt angle corresponds to $[N411i3]^+$.

For the pyrrolidinium imides, a similar case of interference on the peak fitting is present for $[Py13]^+$, resulting in a high tilt angle, and a very large distribution interval. The features corresponding to the $N-CH_3$ vibrations disappear completely starting from [Py14][imide], and the tilt angle reaches a minimum for [Py16][imide], before increasing further for the 10-carbon chain substituent. These results, along with the existence of narrower distributions for the alkylpyrrolidinium imides, suggest that there is a higher ordering at the surface for the aforementioned salts. There is nevertheless some ambiguity regarding the alkylammonium imides, since there are no means to determine which methyl group the r^+ peak is coming from.

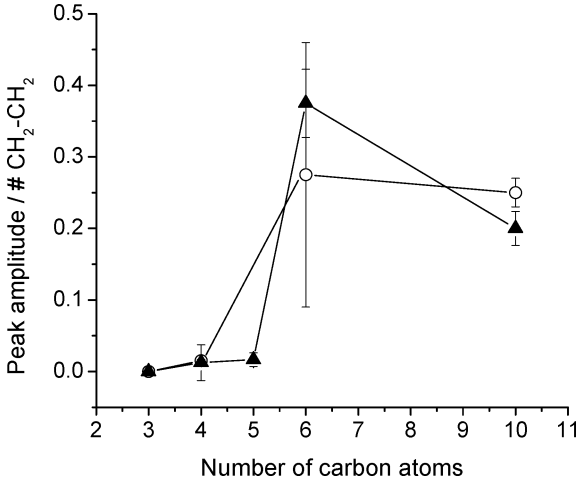

Figure 10. Ratio of d^+ peak amplitude over number of CH2−CH2 bonds in the alkyl chain as a function of the number of carbon atoms for the ammonium (○) and pyrrolidinium imides (▲).

In general, the orientation calculations reveal that the alkyl chain orientation spans an interval from approximately 50 to 70° of tilt from the surface normal, as a function of the alkyl chain length, which is similar to reported values in the literature for imidazolium based ionic liquids.[7,50,61−63] In addition, for the pyrrolidinium case, the very weak d^- vibrations arising from the ring in ssp, along with the absence of any d^+ contribution in sps and pss, suggest that it assumes a position parallel to the surface of the liquid.

Another observation in the sum frequency spectra is the increase in the amplitude of the peaks corresponding to the methylene vibrations as the chain gets longer. The ammonium imides feature an increase in the amplitude of d^+, and d^+_{FR} in ssp, and d^- in the other polarizations. For the pyrrolidinium imides, the growth corresponds to d^+, and d^- in ssp, and d^- in the remaining polarizations. Plots of the amplitude of the methylene symmetric stretch peak (d^+) with the carbon chain length are shown in Figure 9. It is known that the presence of such vibrational modes is an indication of disorder in the alkyl chains due to the presence of kinks, which cause a break in the centrosymmetry within the linear carbon chain which otherwise would lead to the cancellation of the methylene contributions.[40,64] This effect was observed by Iimori et al. for 1-alkyl-3-methylimidazolium tetrafluoroborate ionic liquids.[65] In that work, although the peak amplitude of the symmetric methylene vibration increases with the number of carbons, it is suggested that the probability of a gauche defect per CH_2-CH_2 bond decreases as the alkyl chain length increases, due to an enhancement of the interaction between chains. This was however not observed in the present work, as shown in Figure 10, where the probability increases with the chain length and then decreases for longer chains. Previous observations of this effect were reported for the structure of surfactant monolayers in aqueous solutions in the work of Knock et al.,[66] and Goates et al.,[67] where the enhancement in the strength of the d^+ vibration is attributed to an increase in the conformational disorder, which does not affect the overall orientation of the terminal methyl group. The work of Bell et al.[68] also reports this phenomenon as a function of the surfactant's head group. It is reported that the ratio of strengths of r^+ over d^+ modes (Sr^+/Sd^+) is inversely proportional to the degree of packing, which is dependent on the chemical nature of the head group, being highest for dodecanol and lowest for C_{12}-betaine. A similar dependence was found in this investigation, and is plotted in Figure 11 for both ammonium and pyrrolidinium imides. An

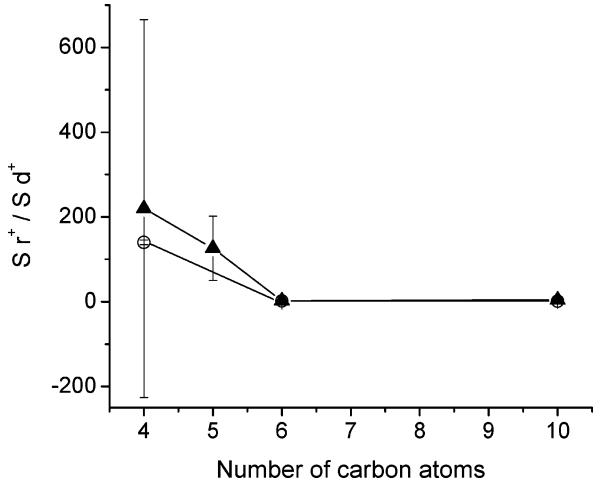

Figure 11. Ratio of strength vibration of r^+ over d^+ versus number of carbons in the alkyl chain for the ammonium (○) and pyrrolidinium imides (▲).

inverse proportionality of (Sr^+/Sd^+) to the degree of packing is observed assuming that the packing of the alkyl chains is proportional to the chain length.

Finally, a comparison may be established between alkylimidazolium and pyrrolidinum based ionic liquids. Even though both groups are chemically different, their overall shape is somewhat similar, since they are characterized by the presence of a ring, and an aliphatic chain substituent. SFG experiments on the gas−liquid interface of alkylimidazolium ionic liquids combined with a variety of anions,[61,69] as well as molecular dynamics simulations,[62,70,71] agree on the fact that the ring lies horizontal to the surface of the liquid, and that the alkyl chain is aligned with the surface normal. Similar remarks were found in the current investigation through the selective deuteration of the butyl chain. In addition, it is observed that the surface structure is dominated by the alkyl chain, once it reaches four carbon units long.

6. Conclusion

The gas−liquid interface of ammonium and pyrrolidinium ionic liquids with varying alkyl chain lengths was studied using sum frequency generation spectroscopy. Unambiguous assignments of the vibrational modes were determined by using compounds with methoxy-terminated and fully deuterated chains, and a more accurate structure of the surface was obtained. In all cases, the longest alkyl chain seems to be pointing upward, and in the case of the pyrrolidinium imides, the ring appears to be lying parallel to the surface of the liquid, in accordance with similar studies of imidazolium based compounds.

The chain length dependence studies suggest that the contribution of the $N-CH_3$ vibration is masked by the chain for lengths of four carbons and more. The ordering at the surface, as pictured by the tilt of the terminal methyl's C_3 symmetry axis, seems to be maximum for the butyl substituted ammonium imide, and for the hexyl substituted pyrrolidinium imide, decreasing for longer chains in every case. Finally, there is an increase in surface disorder proportional to the chain length, as revealed by an enhancement of the methylene peak vibrations, in agreement with previous studies on other ionic liquids.

Acknowledgment. We are grateful for support from the Welch foundation (Grant E1531).

References and Notes

(1) Buzzeo, M. C.; Evans, R. G.; Compton, R. G. *ChemPhysChem* **2004**, *5*, 1106.
(2) Welton, T. *Chem. Rev.* **1999**, *99*, 2071.
(3) Seddon, K. R. *J. Chem. Technol. Biotechnol.* **1997**, *68*, 351.
(4) Sun, J.; Forsyth, M.; MacFarlane, D. R. *J. Phys. Chem. B* **1998**, *102*, 8858.
(5) Golding, J.; Forsyth, S.; MacFarlane, D. R.; Forsyth, M.; Deacon, G. B. *Green Chem.* **2002**, *4*, 223.
(6) Dupont, J.; de Souza, R. F.; Suarez, P. A. Z. *Chem. Rev* **2002**, *102*, 3667.
(7) Aliaga, C.; Santos, C.; Baldelli, S. *Phys. Chem. Chem. Phys.* **2007**, *9*, 3683.
(8) Anderson, J. L.; Dixon, J. K.; Maginn, E. J.; Brennecke, J. F. *J. Phys. Chem. B* **2006**, *110*, 15059.
(9) Anthony, J. L.; Anderson, J. L.; Maginn, E. J.; Brennecke, J. F. *J. Phys. Chem. B* **2005**, *109*, 6366.
(10) Blanchard, L. A.; Gu, Z.; Brennecke, J. F. *J. Phys. Chem. B* **2001**, *105*, 2437.
(11) Sairto, A. M.; Aki, S. N. V. K.; Brennecke, J. F. *J. Am. Chem. Soc.* **2002**, *124*, 10276−10277.
(12) MacFarlane, D. R.; Golding, J.; Forsyth, S.; Forsyth, M.; Deacon, G. B. *Chem. Commun.* **2001**, 1430.
(13) MacFarlane, D. R.; Golding, J.; Forsyth, S.; Forsyth, M.; Deacon, G. B. *Green Chem.* **2002**, *4*, 223.
(14) Matsumoto, H.; Kageyama, H.; Miyasaki, Y. *Chem. Lett.* **2001**, 182.
(15) Matsumoto, H.; Kageyama, H.; Miyasaki, Y. *Chem. Commun.* **2002**, 1726.
(16) Matsumoto, H.; Yanagida, M.; Tanimoto, K.; Nomura, M.; Kitagawa, Y.; Miyasaki, Y. *Chem. Lett.* **2000**, 922.
(17) Anthony, J. L.; Brennecke, J. F.; Holbrey, J. D.; Maginn, E. J.; Mantz, R. A.; Rogers, R. D.; Trulove, P. C.; Visser, A. E.; Welton, T. In *Ionic Liquids in Synthesis*; Wasserscheid, P., Welton, T., Ed.; Wiley-VCH: 2003; p 41.
(18) Mantz, R. A.; Trulove, P. C. In *Ionic Liquids in Synthesis*; Wasserscheid, P., Welton, T., Eds.; Wiley-VCH Verlag: Weinheim, Germany, 2003; p 56.
(19) Sun, J.; Forsyth, M.; MacFarlane, D. R. *Molten Salt Forum* **1998**, *585*, 5−6.
(20) Susan, M. A. B. H.; Noda, A.; Mitsushima, S.; Watanabe, M. *Chem. Commun.* **2003**, 938.
(21) Matsumoto, H.; Matsuda, T.; Miyazaki, Y. *Chem. Lett.* **2000**, *12*, 1430.
(22) Kim, J.; Singh, P.; Shreeve, J. M. *Inorg. Chem.* **2004**, *43*, 2960.
(23) Kim, K.-S.; Choi, S.; Demberelnyamba, D.; Lee, H.; Oh, J.; Lee, B.-B.; Mun, S.-J. *Chem. Commun.* **2004**, 828.
(24) Mazille, F.; Fei, Z.; Kuang, D.; Zhao, D.; Zakeeruddin, S. M.; Gratzel, M.; Dyson, P. J. *Inorg. Chem.* **2006**, *45*, 1585.
(25) MacFarlane, D. R.; Sun, J.; Golding, J.; Meakin, P.; Forsyth, M. *Electrochim. Acta* **2000**, 1271.
(26) MacFarlane, D. R.; Meakin, P.; Sun, J.; Amini, N.; Forsyth, M.; Deacon, G. B. *J. Phys. Chem. B* **1999**, *103*, 4164.
(27) Williams, D. B.; Stoll, M. E.; Scott, B. L.; Costa, D. A.; Oldham, W. J. *Chem. Commun.* **2005**, 1438.
(28) Sun, J.; MacFarlane, D. R.; Forsyth, M. *Ionics* **1997**, *3*, 356.
(29) Trulove, P. C.; Mantz, R. A. In *Ionic liquids in synthesis*; Wasserscheid, P., Welton, T., Eds.; Wiley-VCH Verlag GmbH&Co. KGaA: Weinheim, Germany, 2003; p 103.
(30) MacFarlane, D. R.; Forsyth, S. A.; Golding, J.; Deacon, G. B. *Green Chem.* **2002**, *4*, 223.
(31) Forsyth, M.; Pringle, J. M.; MacFarlane, D. R. In *Electrochemical Aspects of Ionic Liquids*; Ohno, H., Ed.; John Wiley and Sons: Hoboken, NJ, 2005; p 289.
(32) Hilgers, C.; Wasserscheid, P. In *Ionic Liquids in Synthesis*; Wasserscheid, P., Welton, T., Eds.; Wiley-VCH Verlag GmbH&Co. KGaA: Weinheim, Germany, 2003; p 21.
(33) Shen, Y. R. *The Principles of Nonlinear Optics*; John Wiley and Sons: New York, Chichester, Brisbane, Toronto, Singapore, 1984.
(34) Buck, M.; Himmelhaus, M. *J. Vac. Sci. Technol., A* **2001**, *19*, 2717.
(35) Bloembergen, N. *Nonlinear Optics*; W. A. Benjamin Inc.: New York, Amsterdam, 1965.
(36) Aliaga, C.; Baldelli, S. *J. Phys. Chem. B* **2006**, *110*, 18481.
(37) Ward, R. N.; Duffy, D. C.; Davies, P. B.; Bain, C. D. *J. Phys. Chem.* **1994**, *98*, 8536.
(38) Bain, C. D.; Davies, P. B.; Ong, T. H.; Ward, R. N.; Brown, M. A. *Langmuir* **1991**, *7*, 1563.
(39) Bell, G. R.; Benson, S. M.; Bain, C. D. *J. Phys. Chem. B* **1998**, *102*, 218.
(40) Bell, G. R.; Li, Z. X.; Bain, C. D.; Fischer, P.; Duffy, D. C. *J. Phys. Chem. B* **1998**, *102*, 9461.

(41) Snyder, R. G.; Strauss, H. L.; Elliger, C. A. *J. Phys. Chem.* **1982**, *86*, 5145.
(42) Bain, C. D.; Casson, B.; Braun, R. *Chem. Phys. Lett.* **1995**, *245*, 326.
(43) Ong, T. H.; Davies, P. B. *Langmuir* **1993**, *9*, 1836.
(44) Snyder, R. G. *J. Chem. Phys.* **1965**, *42*, 1744.
(45) Strauss, H. L.; Snyder, R. G.; MacPhail, R. A. *J. Phys. Chem.* **1984**, *88*, 334.
(46) Lu, R.; Gan, W.; Wu, B.-H.; Chen, H.; Wang, H.-F. *J. Phys. Chem. B* **2004**, *108*, 7297.
(47) Schettino, V.; Marzocchi, M. P.; Califano, S. *J. Chem. Phys.* **1969**, *51*, 5264.
(48) Evans, J. C.; Wahr, J. C. *J. Chem. Phys.* **1959**, *31*, 655.
(49) Allan, V.; McKean, D. C.; Perchard, J. P.; Josien, M. L. *Spectrochim. Acta* **1971**, *27A*, 1409.
(50) Rivera-Rubero, S.; Baldelli, S. *J. Phys. Chem. B* **2006**, *110*, 4756.
(51) MacPhail, R. A.; Strauss, H. L.; Snyder, R. G.; Elliger, C. A. *J. Phys. Chem.* **1984**, *88*, 334.
(52) Szafranski, C. A.; Tanner, W.; Laibiniz, P. E.; Garrell, R. L. *Langmuir* **1998**, *14*, 3580.
(53) Laibinis, P. E.; Bain, C. D.; Nuzzo, R. G.; Whitesides, G. M. *J. Phys. Chem.* **1995**, *99*, 7663.
(54) Hirose, C.; Akamatsu, N.; Domen, K. *Appl. Spectrosc.* **1992**, *46*, 1051.
(55) Hirose, C.; Akamatsu, N.; Domen, K. *J. Chem. Phys.* **1992**, *96*, 997.
(56) Hirose, C.; Yamamoto, H.; Akamatsu, N.; Domen, K. *J. Phys. Chem.* **1993**, *97*, 10064.
(57) Wang, H.-F.; Lu, R.; Gan, W.; Wu, B.-H.; Chen, H. *J. Phys. Chem. B* **2004**, *108*, 7297.
(58) Wang, H.-F.; Lu, R.; Gan, W.; Wu, B.-H.; Zhang, Z.; Guo, Y. *Int. Rev. Phys. Chem.* **2005**, *24*, 191.
(59) Rao, Y.; Tao, Y.-S.; Wang, H.-F. *J. Chem. Phys.* **2003**, *119*, 5226.
(60) Wang, J.; Paszti, Z.; Even, M. A.; Chen, Z. *J. Am. Chem. Soc.* **2002**, *124*, 7016.
(61) Baldelli, S. *J. Phys. Chem. B* **2003**, *107*, 6148.
(62) Bhargava, B. L.; Balasubramanian, S. *J. Am. Chem. Soc.* **2006**, *128*, 10073.
(63) Lynden-Bell, R. *Mol. Phys.* **2003**, *101*, 2625.
(64) Guyot-Sionnest, P.; Hunt, J. H.; Shen, Y. R. *Phys. Rev. Lett.* **1987**, *59*, 1597.
(65) Iimori, T.; Iwahashi, T.; Kanai, K.; Seki, K.; Sung, J.; Kim, D.; Hamaguchi, H.; Ouchi, Y. *J. Phys. Chem. B* **2007**, *111*, 4860.
(66) Knock, M. M.; Bain, C. D. *Langmuir* **2000**, *16*, 2857.
(67) Goates, S. R.; Schofield, D. A.; Bain, C. D. *Langmuir* **1999**, *15*, 1400.
(68) Bell, G. R.; Bain, C. D.; Ward, R. N. *J. Chem. Soc., Faraday Trans.* **1996**, *92*, 515.
(69) Rivera-Rubero, S.; Baldelli, S. *J. Am. Chem. Soc.* **2004**, *126*, 11788.
(70) Lynden-Bell, R.; Del Popolo, M. *Phys. Chem. Chem. Phys.* **2006**, *8*, 949.
(71) Yan, T.; Li, S.; Jiang, W.; Gao, X.; Xiang, B.; Voth, G. A. *J. Phys. Chem. B* **2006**, *110*, 1800.